Journal of Chromatography A, 1338 (2014) 136–148

Contents lists available at ScienceDirect

Journal of Chromatography A

journal homepage: www.elsevier.com/locate/chroma

# Evaluation and application of static headspace–multicapillary column-gas chromatography–ion mobility spectrometry for complex sample analysis

Chamila J. Denawaka, Ian A. Fowlis, John R. Dean *

*Department of Applied Sciences, Northumbria University, Newcastle upon Tyne NE1 8ST, UK*

ARTICLE INFO

*Article history:*
Received 9 December 2013
Received in revised form 14 February 2014
Accepted 17 February 2014
Available online 25 February 2014

*Keywords:*
Static headspace
Multicapillary column-gas chromatography
Ion mobility spectrometry
Theory
Quantification
Foot malodour

ABSTRACT

An evaluation of static headspace–multicapillary column-gas chromatography–ion mobility spectrometry (SHS-MCC-GC-IMS) has been undertaken to assess its applicability for the determination of 32 volatile compounds (VCs). The key experimental variables of sample incubation time and temperature have been evaluated alongside the MCC-GC variables of column polarity, syringe temperature, injection temperature, injection volume, column temperature and carrier gas flow rate coupled with the IMS variables of temperature and drift gas flow rate. This evaluation resulted in six sets of experimental variables being required to separate the 32 VCs. The optimum experimental variables for SHS-MCC-GC-IMS, the retention time and drift time operating parameters were determined; to normalise the operating parameters, the relative drift time and normalised reduced ion mobility for each VC were determined. In addition, a full theoretical explanation is provided on the formation of the monomer, dimer and trimer of a VC. The optimum operating condition for each VC calibration data was obtained alongside limit of detection (LOD) and limit of quantitation (LOQ) values. Typical detection limits ranged from 0.1 ng bis(methylthio)methane, ethylbutanoate and (E)-2-nonenal to 472 ng isovaleric acid with correlation coefficient ($R^2$) data ranging from 0.9793 (for the dimer of octanal) through to 0.9990 (for isobutyric acid). Finally, the developed protocols were applied to the analysis of malodour in sock samples. Initial work involved spiking an inert matrix and sock samples with appropriate concentrations of eight VCs. The average recovery from the inert matrix was $101 \pm 18\%$ ($n = 8$), while recoveries from the sock samples were lower, that is, $54 \pm 30\%$ ($n = 8$) for sock type 1 and $78 \pm 24\%$ ($n = 6$) for sock type 2. Finally, SHS-MCC-GC-IMS was applied to sock malodour in a field trial based on 11 volunteers (mixed gender) over a 3-week period. By applying the SHS-MCC-GC-IMS database, four VCs were identified and quantified: ammonia, dimethyl disulphide, dimethyl trisulphide and butyric acid. A link was identified between the presence of high ammonia and dimethyl disulphide concentrations and a high malodour odour grading, that is, $\geq 6$. Statistical analysis did not find any correlation between the occurrence of dimethyl disulphide and participant gender.



## 1. Introduction

Ion mobility spectrometry (IMS) was developed in the latter half of the last century in response to the need by the military agencies for a fast and sensitive technique for the detection of chemical warfare agents, explosives, hazardous chemicals and drugs [1–4]. Ion mobility spectrometry and time-of-flight mass spectrometry (TOF-MS) are similar in the sense that ionized compounds are separated on the basis of their charge and size by passage along a tube, the drift tube, under the influence of an electric field. Larger molecules move more slowly than small ones and a spectrum is generated in time, based upon their arrival at the detector. In the case of TOF-MS, it separates fragment ions whereas IMS being a soft ionization technique only generates and separates molecular ions. In contrast to TOF-MS, IMS is an atmospheric technique and as soft ionization is used, only molecular ions of volatile organic compounds need to be resolved. In addition, IMS is not an identification technique, which is a distinct disadvantage over TOF-MS. However, an IMS instrument is compact, ideal for use in the field, relatively simple to operate, sensitive and produces the results very rapidly. Many instruments are now used by the security operations at airports in addition to the military [5].

In recent years, IMS has been combined with chromatographic systems including gas chromatography (GC) [6,7] and liquid chro-

* Corresponding author. Tel.: +44 191 227 3047; fax: +44 191 227 3519.
*E-mail address:* John.Dean@northumbria.ac.uk (J.R. Dean).

http://dx.doi.org/10.1016/j.chroma.2014.02.047

matography mass spectrometry (LC-MS) [8,9] as well as TOF-MS [10,11]. Gas chromatography combined with IMS extends the usefulness of IMS by providing the additional dimension of retention time separation of the gas chromatograph to the drift time separation of the spectrometer. Further, the IMS signal intensity provides quantitative data in addition to the qualitative information.

Currently, very rapid chromatographic separations are carried out using short (up to 25 cm) multicapillary columns (MCC) containing approximately a 1000 parallel capillary tubes coated with a stationary phase. Studies have been carried out to investigate the application of SHS-MCC-GC-IMS [6,7,12,13]. The important operating parameters include gas flows (i.e. drift and carrier gas flows) and temperatures (i.e. drift tube, column and injector) each of which has been studied in order to optimize separation [6,7].

Thus, there are two types of separations: the first is chromatographic separation and the second one is drift separation. Headspace volatile or semi-volatile compounds are selectively separated by the GC column and then introduced into the ionization region of the IMS where they are converted into gas phase ions. Ionization occurs under ambient pressure and in the presence of an applied electric field these generated ions then travel through the drift tube region of the IMS and are detected at the Faraday plate according to their mobility, ion cross section and charge [14,15]. Nitrogen is normally used as both the carrier gas and drift gas. Other gases may also be used but it is a prime requirement that the gas used must contains water [16]. The actual amount does not appear to be critical, and certainly in the case of nitrogen the level is very low (<20 ppm). Detection limits in the IMS are typically in the low ppb range for VCs [13,17].

SHS-MCC-GC-IMS has been used in trace analysis for the characterization of biological and clinical samples [12,18,19], medical diagnosis [13,20], food quality control [6,21], safety monitoring [22], biomolecule analysis [23] and fermentation application [24]. For example, using the static headspace approach, MCC-GC-IMS has been used to differentiate virgin and extra virgin olive oil [6]. These two types of virgin olive oils have very similar characteristics and other analytical techniques are unable to distinguish these selectively. According to the results, static headspace coupled to MCC-GC-IMS provided better results than traditional methods (97% of classification and an 87% prediction were achieved). Perl et al. [7] detected and characterized the metabolic volatile profiles of *Aspergillus fumigatus* and four Candida species by SHS-MCC-GC-IMS. In the study, GC–MS was involved as an additional technique to identify unknowns in the MCC-GC-IMS data. However, isoamyl alcohol and cyclohexanone, which both eluted at similar drift time and retention time, were not resolved by SHS-MCC-GC-IMS. Moreover, the authors [7] have concluded that fast analysis of complex volatile organic compound mixtures without sample preparation or pre-concentration is the major advantage of MCC-GC-IMS [25]. Recently, Jünger et al. [18] conducted similar investigations to identify human pathogenic bacteria by the determination of their characteristic metabolic volatile organic profiles. In the study, SHS-MCC-GC-IMS has been used to differentiate 15 bacterial strains by their metabolic VC profiles. Additionally, time-consuming high-resolution gas chromatography (HRGC)–MS was employed for further confirmation of compounds in several selected strains.

Of interest in this research article is the analysis and identification of VCs associated with malodour from pre- and post-laundry garments, that is, garments before and after the laundry process; specifically small sulphur and nitrogen containing molecules which can be difficult to analyse. Numerous factors have been identified for the formation of malodour in laundries such as humidity, indoor drying, chemical oxidation and metabolism of micro-organisms as well as human odour [26–29]. Human odour is generated from different parts of the body, for example, hair, mouth, foot and axillae, due to bacterial degradation (e.g. large-chain fatty acids that can be broken down by microbes to short-chain, volatile fatty acids). Several investigations have been conducted to investigate the occurrence of axillary odour [30,31]. During wearing, laundry can be contaminated by sebaceous lipids, sweat and dead skin cells. These substrates provide the nourishment and facilitate micro-organism survival on laundries [28,32]. The characteristic malodour is generated from the laundries, which can be identified just after washing due to poor hygiene in laundering. The microbial communities and biofilm which build up inside the washing machine have been identified as sources of malodour with potential for cross-contamination of garments [27,33]. Traditionally in Europe, laundry has been washed at a high temperature (>60 °C). However nowadays, for environmental reasons, lower temperatures are recommended and employed. At lower temperature range (30–40 °C), generation of malodour is more prevalent [27,29]. The use of higher temperature washing conditions decreases the risk of micro-organism survival in laundry compared to lower washing temperatures. Nagoh et al. [28] investigated the odorants generated from the indoor drying of garments and identified numerous odorant compounds such as medium-chain alcohols, medium-chain aldehydes, ketones, fatty acids, N-compounds and S-compounds. Munk et al. [32] investigated the compounds attached to laundry soiled with sweat and sebum just after a washing process. Under mild washing condition (low temperature), they identified 14 different odorants, specifically, ethyl-2-methylpropanoate, ethylbutanoate,1-hexen-3-one, 1-octen-3-one, (Z)-4-heptenal, octanal, (E)-2-octenal, methional, (Z)-2- nonenal, (E,Z)-2,6-nonadienal, (E,Z)-2,4-nonadienal, (E,E)-2,4-decadienal, 4-methoxybenzaldehyde.

Adhesion of odorants to different textiles has also been investigated. The determination of how well-selected odorants adhere to cotton and polyester textiles during laundry and the drying process was carried out by Munk et al. [27]. According to their study, odorants were more effectively removed from cotton textiles rather than polyesters during the wash cycle. The removal ability of odorants from textiles is dependent on the hydrophobicity and hydrophilicity of the textile; the hydrophobicity of polyester fabric preventing odorant removal. Conversely, the odour generated in cotton during wet storage was significantly higher than in polyester [27]. This may be caused by the greater water absorbency of (or hydrophilicity) cotton fibres over polyester fibres.

The overall aim of this article was to evaluate the performance of SHS-MCC-GC-IMS for the analysis of volatile compounds in complex matrices. This was achieved by: (a) development of a hypothesis on the formation of analyte monomers, dimers and trimers, (b) investigation of the main operating parameters and their influence on signal, (c) development of a strategy for calibration of VCs on different columns, that is, polar and non-polar and (d) application of the developed methodology to the analysis of foot malodour, specifically socks.

## 2. Experimental

### 2.1. Chemicals/Reagents

Acetone (CAS 67-64-1, ≥ 99.9%), ammonia (CAS 1336-21-6, 28% $NH_3$ in $H_2O$, ≥ 99.99%), bis(methylthio)methane (CAS 1618-26-4, 99%), 1- butanethiol (CAS 109-79-5, 99%), butyric acid (CAS 107-92-6, ≥ 99%), (E,E)-2,4-decadienal (CAS 25152-84-5, ≥ 85%), 1-decanol (CAS 112-30-1, 99%), dimethyl disulphide (CAS 624-92-0, ≥ 98%), dimethyl sulphide (CAS 75-18-3, ≥ 99%), dimethyl trisulphide (CAS 3658-80-8, ≥ 98%), 1-dodecanol (CAS 112-53-8, 98%), ethanethiol (CAS 75-08-1, 97%), ethylbutanoate (CAS 105-54-4, ≥ 98%), 4-fluoroacetophenone (CAS 403-42-9, 99%), guaiacol

(2-methoxy phenol) (CAS 90-05-1, ≥ 98%), hexanoic acid (CAS 142-62-1, ≥ 99.5%), isobutyric acid (CAS 79-31-2, 99%), isovaleric acid (CAS 503-74-2, 99%), methional (CAS 3268-49-3, ≥ 97%), 4-methoxybenzaldehyde (CAS 123-11-5, 98%), 3-methylindole (CAS 83-34-1, 98%), (E,E)-2,4-nonadienal (CAS 5910-87-2, ≥ 85%), 2-nonanone (CAS 821-55-6, ≥ 98%), (E)-2-nonenal (CAS 18829-56-6, 97%), octanal (CAS 124-13-0, 99%), (E)-2-octenal (CAS 2548-87-0, ≥ 94%), 2-phenylethanol (CAS 60-12-8, ≥ 99%), propionic acid (CAS 79-09-4, ≥ 99.5%), 2-propanethiol (CAS 75-33-2, ≥ 98%), triethylamine (CAS 121-44-8, 99%), trimethylamine (CAS 75-50-3, ≥ 99%), 2-undecanone (CAS 112-12-9, 99%) and valeric acid (CAS 109-52-4, ≥ 99%). Stock solutions (10,000 ppm) were prepared using acetone. Ultra-164 pure water of conductivity 18.2 MΩ cm was produced by a direct QTM Millipore system 165 (Molsheim, France) and was used in all dilution steps.

Sock samples (sock type 1: 74% cotton, 19% polyester, 5% nylon and 2% lycra; sock type 2: 74% cotton, 25% polyester and 1% elastane) were obtained from a local retail outlet (Newcastle, UK). Headspace (20 mL) crimp-cap vials and magnetic caps were purchased from Sage Analytical Ltd (Lancashire, UK). Nylon Fire Bags (250 mm × 375 mm) were obtained from Crime Scene Investigation (Woburn Sands, UK) and were used for collection and storage of the soiled fabric samples.

### 2.2. Instrumentation

A FlavourSpec SHS-MCC-GC-IMS instrument manufactured by G.A.S.-Gesellschaft für Analytische Sensorsysteme mbH (Dortmund, Germany), Fig. 1, was used throughout this project. The SHS-MCC-GC-IMS was fitted with an automatic sampler unit (CTC-PAL, CTC Analytics AG, Zwingen, Switzerland), and utilised a heated air-tight syringe. An MCC (Multichrom, Novosibirsk, Russia) was used for the chromatographic separation. The MCC comprises a stainless steel tube, 20 cm × 3 mm ID, containing approximately 1000 parallel capillary tubes, 40 μm ID, coated with 0.2 μm film thickness of stationary phase, that is, OV-5 or Carbowax 20M. Atmospheric pressure ionisation is generated by a Tritium ($^3$H) solid state bonded source ($\beta$-radiation, 300 MBq with a half-life of 12.5 years). The IMS has a drift tube length of 50 mm. Separation in the IMS drift tube is achieved by applying an electric field of 2 kV to the ionized volatiles in a pulsed mode using an electronic shutter opening time of 100 μs. The drift gas was $N_2$ (99.998%) with a drift pressure of 101 kPa (ambient pressure). All data are acquired in the positive ion mode and each spectrum is formed with the average of 42 scans. All data, determined as peak height, against *x* and *y* co-ordinates per VC, are processed using the LAV software (version 2.0.0 from G.A.S). The software package enables both two- and three-dimensional data visualisation plots.

### 2.3. Procedure for Foot Malodour

Eleven healthy volunteers were selected to participate in the study. Each participant received a pair of new socks and a wear protocol; each sock was enclosed in a uniquely coded sample bag, that is, right sock and left sock. The wear protocol was as follows: each foot was to be rinsed thoroughly with tap water and then dried. Participants were not allowed to apply odorous products during the study, that is, deodorant or moisturiser. Participants then wore the socks over a minimum period of 10 h during one day in whatever footwear was appropriate, for example, shoes. After the specified time period, the participants transferred each sock into the uniquely coded bag, sealed and stored overnight in a dark place. The sample containing bags were then returned to the investigator the following day. Participants completed a questionnaire which identified their type of footwear in which the sock was worn and also the level of physical activity undertaken. The whole process was repeated over three weeks. Each week, the odour associated with each sock/participant was assessed for malodour by a trained assessor. Each sample was graded according to a numerical scale ranging from 0 (no malodour) to 10 (malodorous).

The socks were then sub-sampled (Fig. 2) in three distinct areas, that is, toes, ball and heel by taking approximately 0.5 g of material accurately weighed. The sub-samples were then placed into 20 mL headspace vial and closed with a magnetic cap prior to SHS-MCC-GC-IMS analysis. Unworn socks were prepared as blank samples and analysed using the same methods; this allowed extraneous VCs to be identified and eliminated from future data treatment.

## 3. Results and Discussion

### 3.1. Theory of IMS Ionization Process

The IMS uses an atmospheric pressure ionization process. Nitrogen or air may be used as carrier and drift gasses, but it is essential that they contain a concentration of water in order for the ionization process to take place. The chemistry of the ionization process is generally not well presented in the literature. This discussion will attempt to rectify that situation by providing a logical series of essentially balanced chemical equations which adequately describe the formation of the reactant ion or the formation of dimers and trimers. Typically, the general explanation of the IMS process presented in most publications is as follows [34]. Fast electrons from the tritium $\beta$-radiation source react with the water molecules to form reactant ions described as $H^+(H_2O)_n$. Soft chemical ionization of the analyte molecules by the reactant ions generates protonated species, which are separated on the basis of their mass, shape, size and charge by the electric field in the drift tube. Equations frequently presented in the literature to describe the ionization process are shown below.

$$N_2 \rightarrow \beta \rightarrow N_2^+ + e^- \quad (1)$$

$$N_2^+ + (H_2O) \rightarrow H^+(H_2O) \quad (2)$$

The product of this reaction is generally called the reactant ion. It is then suggested that the reactant ion reacts with an analyte molecule as follows:

$$M + H^+(H_2O) \rightarrow M^+(H_2O) \quad (3)$$

It is said that this reaction yields the protonated monomer, however, the appearance and disappearance of protons are not adequately explained nor the rationale for the formation of subsequent dimers and trimers presented. Since, as stated earlier, this is a soft ionization process, fragmentation of ions does not take place but dimers and trimers occur frequently and can be an aid to compound identification. This simplistic representation of the chemistry above does not take into account that we are dealing with clusters of water molecules rather than individuals. It has been reported [35,36] that it is common to find at least 20 water molecules in association with each other, although larger and smaller aggregates are also common. It has been postulated [35] that when water becomes protonated, the protonated molecule, the hydroxonium ion, $H_3O^+$, is on the outside of the cluster with the charge facing outwards. The following is a hypothesis which will attempt to explain, more comprehensively, the mechanism for the formation of the reactant ion and the subsequent formation of the monomer and possible dimer and trimer and which could account for phenomena detected on the topographical displays. The following steps are therefore proposed:

*Step 1*. The formation of the reactant ion from water and nitrogen in the presence of the $\beta$ radioactive source could proceed as follows.

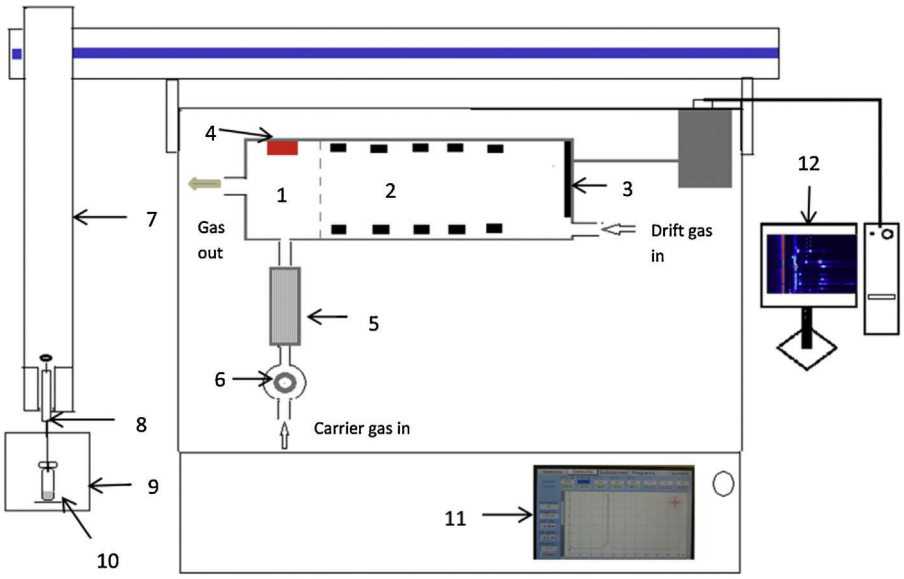


**(1) ionisation region; (2) drift region; (3) detector (Faraday plate); (4) radiation source; (5) multi-capillary column; (6) injector; (7) robotic arm; (8) syringe; (9) incubator; (10) sample vial (11) integral display; (12) PC.**

**Fig. 1.** Schematic diagram of SHS-MCC-GC-IMS. (1) Ionisation region; (2) drift region; (3) detector (Faraday plate); (4) radiation source; (5) multicapillary column; (6) injector; (7) robotic arm; (8) syringe; (9) incubator; (10) sample vial; (11) integral display; (12) PC.

This generates the reactant ion peak (RIP) on the topographical display.

$$N_2 \rightarrow \beta^- \rightarrow N_2^+ + e^- \quad (4)$$

$$N_2^+ + (H_2O)_m \rightarrow H^+(H_2O)_{m-1}(N_2)_n + OH^- + N_2 \quad (5)$$

The hydroxyl ion will depart with the drift gas and will not be detected by the instrument (Note: Since nitrogen is present in very large excess it may be disregarded in the subsequent equation series). The resulting ion can now rearrange to generate the hydroxonium ion which better represents the nature of the reactant ion.

$$H^+(H_2O)_{m-1} = H_3O^+(H_2O)_{m-2} \quad (6)$$

We believe that the hydroxonium ion is the key to the understanding of the chemistry involved in the generation of monomers, dimers and trimers as is shown in the following equations.

*Step 2*. The reactant ion in the presence of an analyte molecule (M) now forms a protonated monomer and liberates a neutral water molecule.

$$M + H_3O^+(H_2O)_{m-2} \rightarrow MH^+(H_2O)_{m-2} + H_2O \quad (7)$$

The elimination of a neutral water molecule is a logical by-product of the reaction.

*Step 3*. Now follows a charge transfer step whereby one of the associated water molecules becomes protonated to generate a new hydroxonium ion containing product monomer ion.

$$MH^+(H_2O)_{m-2} = MH_3O^+(H_2O)_{m-3} \quad (8)$$

*Step 4*. The charge transfer product now reacts with a further molecule of analyte to yield a protonated dimer and neutral water.

$$M + MH_3O^+(H_2O)_{m-3} \rightarrow M_2H^+(H_2O)_{m-3} + H_2O \quad (9)$$

*Step 5*. Then may follow a further charge transfer step as described above in Step 3 (Eq. (8)).

$$M_2H^+(H_2O)_{m-3} = M_2H_3O^+(H_2O)_{m-4} \quad (10)$$

*Step 6*. Again the charge transfer product reacts with another analyte molecule to form a protonated trimer and neutral water.

$$M + M_2H_3O^+(H_2O)_{m-4} \rightarrow M_3H^+(H_2O)_{m-4} + H_2O \quad (11)$$

On the basis of the hypothesis above, it may be possible that product ions containing four or even more analyte entities may be formed under favourable conditions. However, how the resulting charge on the product ions is distributed is clearly a matter for speculation. An example of the typical topographical output showing the presence of a monomer, dimer and trimer is shown in Fig. 3. On the *x*-axis is the IMS drift separation in which it is

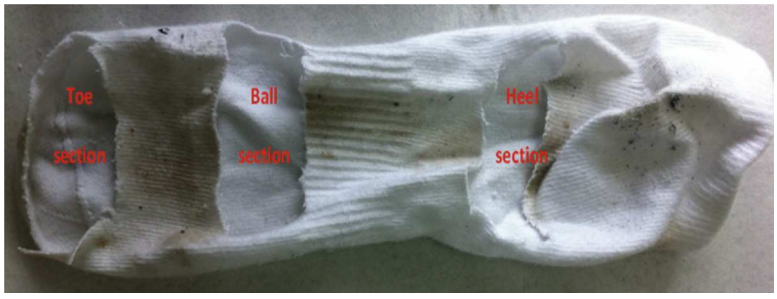


**Fig. 2.** Sectioning of sample for sock malodour study.

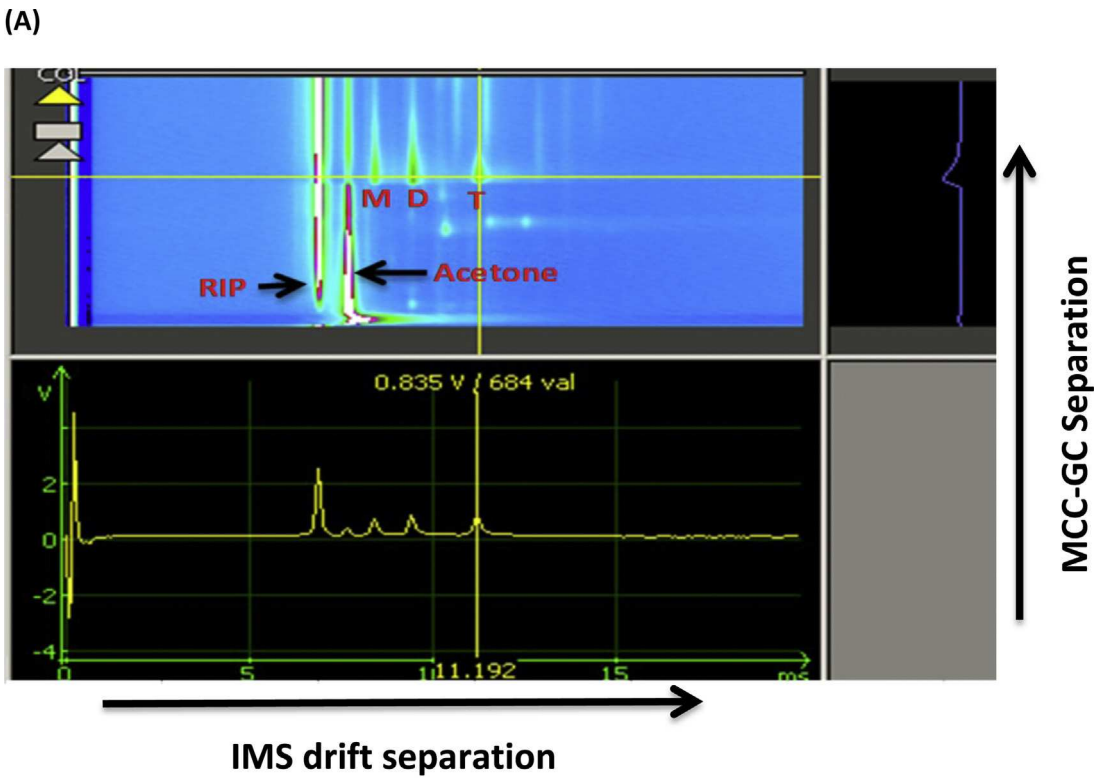


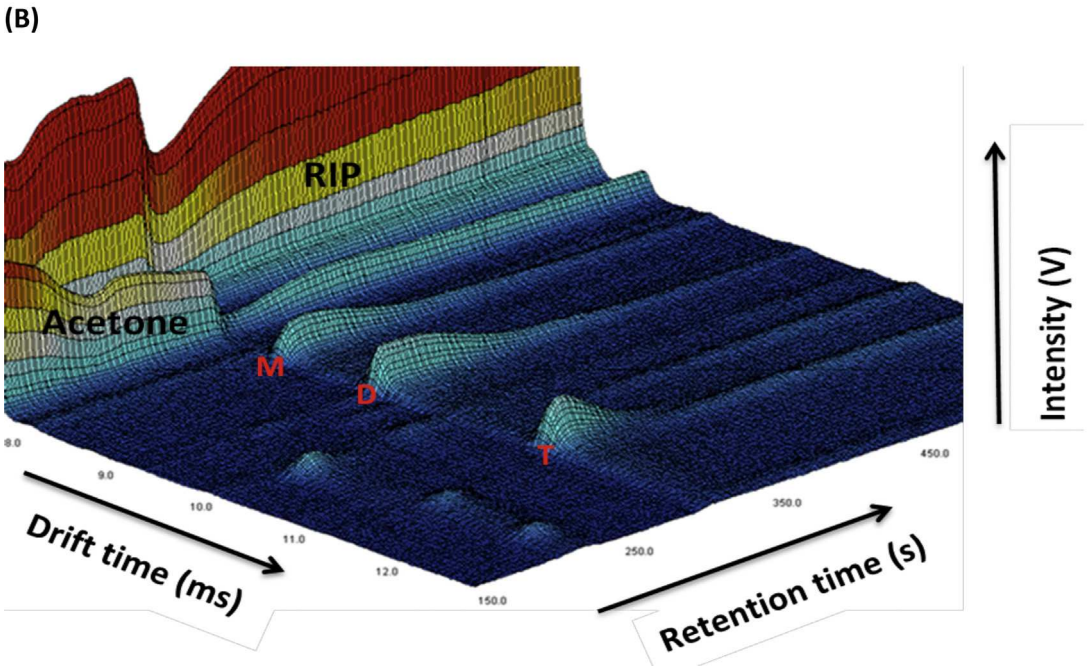


**Fig. 3.** 2D (A) and 3D (B) data visualisation in SHS-MCC-GC-IMS: Example topographic view for the formation of monomer (M), dimer (D) and trimer (T) for 4-fluoracetophenone (250 ng).

possible to identify (from left to right) the RIP, monomer, dimer and trimer for 4-fluoroacetophenone, whereas on the *y*-axis the MCC-GC separation for 4-fluoroacetophenone is apparent.

### 3.2. Method Optimization and IMS Database Generation

The approach to method development was initially based on a trial and error approach until sufficient experience was gained to be able to systematically separate and analyse the 32 VCs. In the initial method development stages, a range of VCs were analysed on the polar (Carbowax-20M) column. However, it was found in most cases that the compounds were eluted with very short retention times, with the exception of ammonia, 1-decanol, 1-dodecanol, guaicaol, 4-methoxybenzaldehyde and 2-phenylethanol. On that basis and to obtain better chromatographic separation and avoid co-elution of compounds, the non-polar (OV-5) column was also investigated. Since many of the compounds of interest have a significant alkyl content, it was reasonable to suppose that these would

**Table 1**
Experimental conditions for all the volatile compounds analysed by the SHS-MCC-GC-IMS.

| Column type | COMPOUNDS | Incubation conditions | | MCC-GC conditions | | | | | IMS conditions | |
|---|---|---|---|---|---|---|---|---|---|---|
| | | Incubation time (min) | Incubation temperature (°C) | Syringe temperature (°C) | Injection temperature (°C) | Injection volume (mL) | Column temperature (°C) | Carrier gas flow (mL min$^{-1}$) | IMS temperature (°C) | Drift gas flow (mL min$^{-1}$) |
| Carbowax 20M | Ammonia [a] | 10 | 95 | 95 | 80 | 2.2 | 35 | 10 | 60 | 500 |
| Carbowax 20M | 1-Dodecanol<br>Guaiacol<br>4-Methoxybenzaldehyde<br>2-Phenylethanol | 5 | 95 | 85 | 80 | 1.5 | 70 | 150 | 45 | 500 |
| Carbowax 20M | 1-decanol | 5 | 95 | 85 | 80 | 1.5 | 30 | 150 | 45 | 500 |
| OV-5 | 1-Butanethiol<br>Ethylbutanoate<br>4-Fluoracetophenone<br>(E,E)-2,4-Nonadienal<br>2-Nonanone (E)-2-Nonenal<br>Octanal<br>(E)-2-Octenal<br>2-Undecanone | 5 | 95 | 85 | 80 | 1.5 | 30 | 150 | 45 | 500 |
| OV-5 | (E,E)-2,4-Decadienal<br>3-Methylindole | 5 | 95 | 85 | 80 | 1.5 | 70 | 150 | 45 | 500 |
| OV-5 | Bis(methylthio)methane<br>Butyric acid<br>Dimethyl disulphide Dimethyl sulphide Dimethyl trisulphide<br>Ethanethiol<br>Hexanoic acid<br>Isobutyric acid<br>Isovaleric acid<br>Methional<br>Propionic acid<br>2-Propanethiol<br>Triethylamine<br>Trimethylamine<br>Valeric acid | 5 | 95 | 85 | 80 | 1.5 | 35 | 10 | 60 | 500 |

[a] Sample volume 2 mL (for all other compounds the sample volume was 0.1 mL)

**(A)** (i) Column type: Carbowax 20M; column temp 35 $^0$C; carrier gas flow 10 mL min$^{-1}$ and drift temp 60 $^0$C

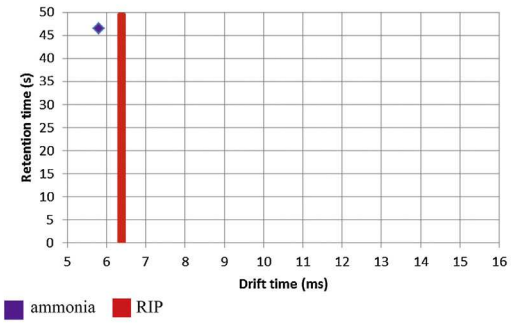


(ii) Column type: Carbowax 20M; column temp 70 $^0$C; carrier gas flow 150 mL min$^{-1}$ and drift temp 45 $^0$C

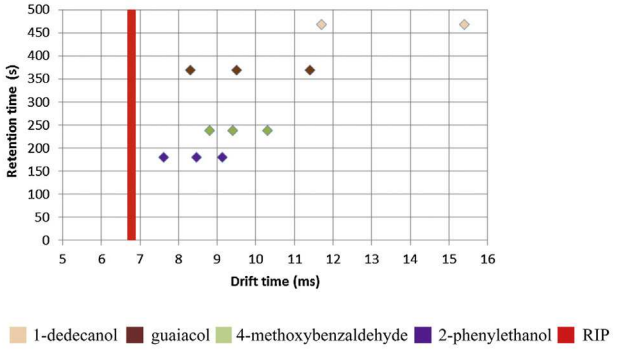


(iii) Column type: Carbowax 20M; column temp 30 $^0$C; carrier gas flow 150 mL min$^{-1}$ and drift temp 45 $^0$C

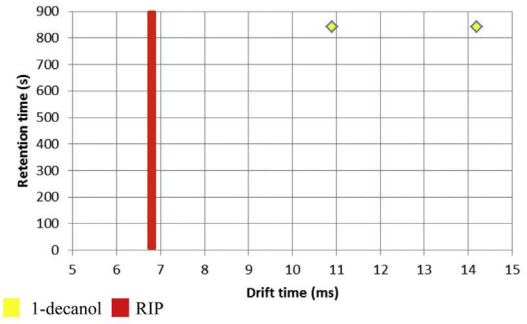


**(B)** (i) Column type: OV-5; column temp 30 $^0$C; carrier gas flow 150 mL min$^{-1}$ and drift temp 45 $^0$C

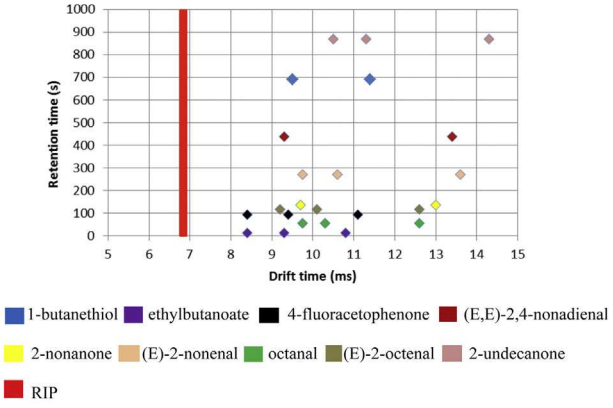


(ii) Column type: OV-5; column temp 70 $^0$C; carrier gas flow 150 mL min$^{-1}$ and drift temp 45 $^0$C

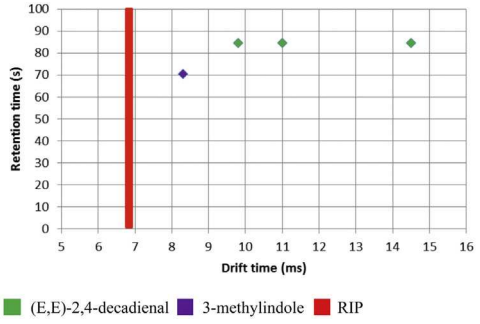


(iii) Column type: OV-5; column temp 35 $^0$C; carrier gas flow 10 mL min$^{-1}$ and drift temp 60 $^0$C

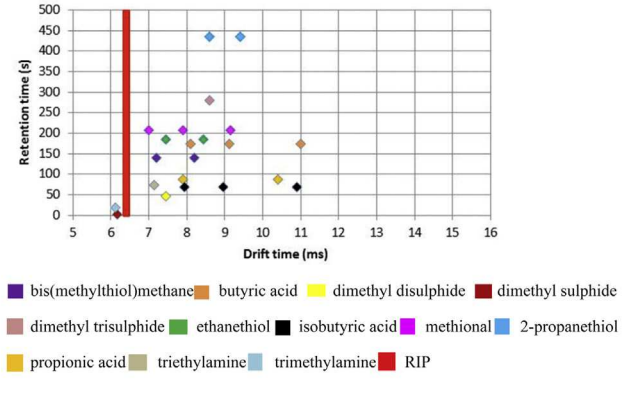


(iv) Column type: OV-5; column temp 35 $^0$C; carrier gas flow 10 mL min$^{-1}$ and drift temp 60 $^0$C

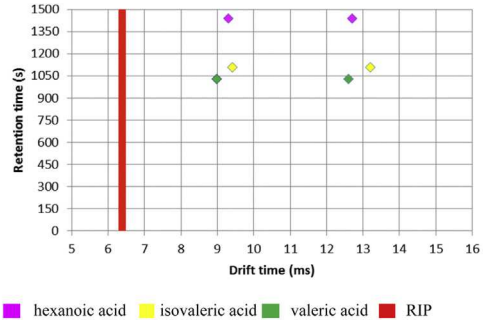


**Fig. 4.** Two-dimensional maps of VCs separated by either the (A) Carbowax 20M column or (B) OV-5 column. (A) (i) Column type, Carbowax 20M; column temp, 35 °C; carrier gas flow, 10 mL min$^{-1}$ and drift temp, 60 °C. (ii) Column type, Carbowax 20M; column temp, 70 °C; carrier gas flow, 150 mL min$^{-1}$ and drift temp, 45 °C. (iii) Column type, Carbowax 20M; column temp, 30 °C; carrier gas flow, 150 mL min$^{-1}$ and drift temp, 45 °C. (B) (i) Column type, OV-5; column temp, 30 °C; carrier gas flow, 150 mL min$^{-1}$ and drift temp, 45 °C. (ii) Column type, OV-5; column temp, 70 °C; carrier gas flow, 150 mL min$^{-1}$ and drift temp, 45 °C. (iii) Column type, OV-5; column temp, 35 °C; carrier gas flow, 10 mL min$^{-1}$ and drift temp, 60 °C. (iv) Column type, OV-5; column temp, 35 °C; carrier gas flow, 10 mL min$^{-1}$ and drift temp, 60 °C.

be better resolved by OV-5 phase which consists predominantly of alkyl groups. Firstly, the key experimental variables of the MCC-GC-IMS were optimised in order to obtain a better separation and maximise sensitivity and selectivity for the chosen VCs. The most important variables influencing the separation process were identified as the carrier gas flow rate, the multicapillary GC column oven temperature and the drift gas flow rate. Using a univariate optimisation approach, each variable was systematically investigated for all 32 VCs on the two column types. Using this approach, it was found, in general terms, that a high column temperature and a high carrier gas flow rate eluted the VCs rapidly. Conversely, a lower carrier gas flow rate and column temperatures increased retention time. Also, of the two variables altering the column temperature was the most effective way to change the retention time. In contrast, the drift gas flow rate did not significantly influence the drift time. However, the combined effect of the drift gas flow rate and carrier gas flow rate influenced the intensity and sharpness of the RIP. As the intensity of the RIP is the major contributor that influences the sensitivity of the detected VCs, it is important that the drift gas is therefore also optimised. It was also found that the drift gas flow rate had a significant influence on memory effects and carry-over; generally a higher drift gas flow rate resulted in lower memory effects and carry-over between injections. As the maximum injector temperature was 80 °C, this was used throughout the study to avoid condensation of VCs in the injector and connecting tubing. In addition to the SHS-MCC-GC-IMS parameters, it was also necessary to consider the sample introduction parameters of sample incubation time and temperature as well as the injection volume. It was found that the intensity of the VC peaks increased with both sample incubation time and temperature (Note: it was subsequently found in the sample fabric analysis that increased sample incubation time and temperature led to an increased background); the optimized operating conditions for incubation time and temperature were therefore determined as 5 min and 95 °C, respectively, with a fixed injection volume of 1.5 mL for 31 VCs (Note: the exception was ammonia for which a longer incubation time (10 min) and a higher injection volume (2.2 mL) were required). The experimental conditions for the separation of all 32 VCs are shown in Table 1. Using the LAV software, it is possible to generate two-dimensional maps of the VC analysed under standardised operating conditions as a guide to the identification of compounds in unknown samples, thereby creating an initial VC database per standard operating conditions. It is also possible to generate three-dimensional presentations of the data. The two-dimensional VC maps are shown in Fig. 4. Fig. 4(A) shows the separations on the Carbowax 20M column for (i) ammonia (monomer only), (ii) 1-dodecanol (monomer and dimer), guaiacol (monomer, dimer and trimer), 4-methoxybenzaldehyde (monomer, dimer and trimer) and 2-phenylethanol (monomer, dimer and trimer), (iii) for 1-decanol (monomer and dimer) while Fig. 4(B) shows the separations on the OV-5 column for (i) 1-butanethiol (monomer and dimer), ethylbutanoate (monomer, dimer and trimer), 4-fluoroacetophenone (monomer, dimer and trimer), (E,E)-2,4-nonadienal (monomer and dimer), 2-nonanone (monomer and dimer), (E)-2-nonenal (monomer, dimer and trimer), octanal (monomer, dimer and trimer), (E)-2-octenal (monomer, dimer and trimer) and 2-undecanone (monomer, dimer and trimer) (ii) (E,E)-2,4-decadienal (monomer, dimer and trimer) and 3-methylindole (monomer only), (iii) bis(methylthio)methane (monomer and dimer), butyric acid (monomer, dimer and trimer), dimethyl disulphide (monomer only), dimethyl sulphide (monomer only), dimethyl trisulphide (monomer only), ethanethiol (monomer and dimer), isobutyric acid (monomer, dimer and trimer), methional (monomer, dimer and trimer), 2-propanethiol (monomer and dimer), propionic acid (monomer and dimer), triethylamine (monomer only) and trimethylamine (monomer only) and (iv) hexanoic acid (monomer and dimer), isovaleric acid (monomer and dimer) and valeric acid (monomer and dimer) (Note: hexanoic acid, isovaleric acid and valeric acid were determined under the same conditions as those for compounds in Fig. 4(B) (iii); they are provided as Fig. 4(B) (iv) to allow a scale adjustment to take place).

As indicated, drift time and retention time are the important parameters for the reliable identification of unknown VCs. However, in order to minimise instrument variation, for example, the effects of pressure and temperature, a normalisation term has been defined, namely the relative drift time, $t_{rd}$ [37,38]. The relative drift time can be calculated using the following equation.

$$t_{rd} = \frac{t_d}{t_{dRIP}} \tag{12}$$

where $t_d$ is the measured drift time of the VC and $t_{dRIP}$ is the drift time of the RIP. In this case, the RIP is considered as an internal standard that compensates for any instrument variation. According to Eq. (12), the relative drift time of the RIP ($t_{rdRIP}$) is always assumed to be equal to 1. However, VC clusters which have a drift velocity greater than that of the ionised water cluster have a $t_{rd}$ of < 1 while those with a velocity lower than the water cluster appear at higher relative drift time ($t_{rd}$ > 1). In this study, as indicated above, different experimental parameters were employed to analyse a wide variety of VCs. Therefore, the introduction of a parameter which is independent of experimental conditions and is characteristic of a particular VC is invaluable (Table 2).

In addition to the relative drift time, it is also important to be able to identify a separated VC based on its reduced ion mobility. The determination of the reduced ion mobility allows a reduction in the environmental and instrumental influences on the VC. In practice the reduced ion mobility is derived from the drift time of the VC which is then normalised to the applied electric field, the length of the drift region and the temperature and pressure of the drift gas [12]. However, Vautz et al. [12] modified the traditional approach for the calculation of the reduced ion mobility and identified a new term 'Ko normalised'; this represents the calculation of the reduced ion mobility relative to the RIP (internal standard). However, this approach assumes that the drift time of the RIP is constant and does not vary. For example, the experimentally reported value for the reduced ion mobility as 2.06 $cm^2\,V^{-1}\,s^{-1}$ for the positive RIP and 2.22 $cm^2\,V^{-1}\,s^{-1}$ for the negative RIP based on extensive verification over many years [12]. If the experimentally derived RIP is not known with any certainty then it must be calculated per VC as was the case in this work.

The normalised reduced ion mobility (Ko normalised, $cm^2\,V^{-1}\,s^{-1}$) for the RIP was calculated as follows (using Eq. (13)):

$$Ko_{(RIP)} = \left[\left(\frac{L^2}{E \times t_{dRIP)}}\right) \times \left(\frac{P}{P_0}\right) \times \left(\frac{T_0}{T}\right)\right] \tag{13}$$

where $L$ is the length of the drift region (cm), $E$ is the electrical field strength (V), $t_{dRIP}$ is the drift time (ms) of the RIP, $P$ is the pressure of the drift gas (hPa), $P_0$ is the standard atmospheric pressure (1013.2 hPa), $T$ is the temperature of the drift gas (K), and $T_0$ is the standard temperature (273.2 K).

Once the $Ko_{(RIP)}$ values have been experimentally determined, the normalised reduced ion mobility (Ko) for the VCs, in units of $cm^2\,V^{-1}\,s^{-1}$, can be calculated as follows:

$$Ko_{(VC)} = \frac{F_{IMS}}{t_{D(VC)}} \tag{14}$$

where $F_{IMS}$ is the IMS factor ($cm^2\,V^{-1}$) derived as follows: $F_{IMS} = Ko_{(RIP)} \cdot t_{dRIP}$ and $t_{D(VC)}$ is the drift time (ms) of the VC. The derived normalised reduced ion mobilities for the VCs are shown in Table 2 (Note: The average value for the reduced ion mobility of the

**Table 2**
Compound identification by SHS-MCC-GC-IMS.

| Compound | Column type | Compound cluster | Retention time (s) Mean ± SD ($n$ = 3) | Drift time (ms) Mean ± SD ($n$ = 3) | Relative drift time Mean ± SD ($n$ = 3) | Normalised reduced ion mobility ($cm^2\ V^{-1}\ S^{-1}$) Mean ± SD ($n$ = 3) |
|---|---|---|---|---|---|---|
| Ammonia | Carbowax 20M | Monomer | 46.4 ± 7.2 | 5.81 ± 0.00 | 0.90 ± 0.00 | 2.62 ± 0.00 |
| Bis(methylthio)methane | OV-5 | Monomer | 140 ± 2 | 7.20 ± 0.00 | 1.12 ± 0.00 | 2.11 ± 0.00 |
| | | Dimer | | 8.26 ± 0.00 | 1.28 ± 0.00 | 1.84 ± 0.00 |
| 1-Butanethiol | OV-5 | Monomer | 703 ± 4 | 9.69 ± 0.40 | 1.40 ± 0.02 | 1.57 ± 0.01 |
| | | Dimer | | 11.6 ± 0.00 | 1.67 ± 0.02 | 1.31 ± 0.00 |
| Butyric acid | OV-5 | Monomer | 174 ± 2 | 8.16 ± 0.00 | 1.27 ± 0.00 | 1.87 ± 0.00 |
| | | Dimer | | 9.12 ± 0.04 | 1.42 ± 0.01 | 1.67 ± 0.01 |
| | | Trimer | | 11.0 ± 0.00 | 1.72 ± 0.00 | 1.39 ± 0.00 |
| (E,E)-2,4-Decadienal | OV-5 | Monomer | 84.6 ± 4.7 | 9.84 ± 0.04 | 1.42 ± 0.01 | 1.10 ± 0.01 |
| | | Dimer | | 11.0 ± 0.04 | 1.58 ± 0.01 | 0.99 ± 0.00 |
| | | Trimer | | 14.5 ± 0.00 | 2.09 ± 0.00 | 0.75 ± 0.00 |
| 1-Decanol | Carbowax 20M | Monomer | 842 ± 6 | 10.9 ± 0.00 | 1.60 ± 0.00 | 0.99 ± 0.00 |
| | | Dimer | | 14.2 ± 0.00 | 2.08 ± 0.00 | 0.76 ± 0.00 |
| Dimethyl disulphide | OV-5 | Monomer | 46.4 ± 0.60 | 7.45 ± 0.00 | 1.15 ± 0.00 | 2.05 ± 0.00 |
| Dimethyl sulphide | OV-5 | Monomer | 2.36 ± 0.57 | 6.17 ± 0.01 | 0.96 ± 0.00 | 2.47 ± 0.00 |
| Dimethyl trisulphide | OV-5 | Monomer | 280 ± 6 | 8.60 ± 0.04 | 1.32 ± 0.01 | 1.77 ± 0.01 |
| 1-Dodecanol | Carbowax 20M | Monomer | 468 ± 4 | 11.7 ± 0.04 | 1.71 ± 0.00 | 0.92 ± 0.00 |
| | | Dimer | | 15.4 ± 0.04 | 2.26 ± 0.00 | 0.70 ± 0.00 |
| Ethanethiol | OV-5 | Monomer | 185 ± 3 | 7.45 ± 0.00 | 1.15 ± 0 .00 | 2.05 ± 0.00 |
| | | Dimer | | 8.44 ± 0.00 | 1.31 ± 0.00 | 1.81 ± 0.00 |
| Ethylbutanoate | OV-5 | Monomer | 12.7 ± 0.6 | 8.39 ± 0.04 | 1.20 ± 0.01 | 1.29 ± 0.01 |
| | | Dimer | | 9.27 ± 0.00 | 1.33 ± 0.00 | 1.17 ± 0.00 |
| | | Trimer | | 10.8 ± 0.00 | 1.55 ± 0.00 | 1.00 ± 0.00 |
| 4-Fluoracetophenone | OV-5 | Monomer | 93.7 ± 1.6 | 8.38 ± 0.00 | 1.22 ± 0.01 | 1.29 ± 0.00 |
| | | Dimer | | 9.37 ± 0.00 | 1.36 ± 0.01 | 1.15 ± 0.00 |
| | | Trimer | | 11.2 ± 0.00 | 1.62 ± 0.01 | 0.97 ± 0.00 |
| Guaiacol | Carbowax 20M | Monomer | 180 ± 1 | 7.61 ± 0.00 | 1.11 ± 0.00 | 1.42 ± 0.00 |
| | | Dimer | | 8.46 ± 0.04 | 1.23 ± 0.01 | 1.28 ± 0.01 |
| | | Trimer | | 9.13 ± 0.00 | 1.33 ± 0.00 | 1.18 ± 0.00 |
| Hexanoic acid | OV-5 | Monomer | 1439 ± 6 | 9.29 ± 0.00 | 1.43 ± 0.00 | 1.64 ± 0.00 |
| | | Dimer | | 12.7 ± 0.04 | 1.96 ± 0.01 | 1.20 ± 0.00 |
| Isobutyric acid | OV-5 | Monomer | 68.9 ± 4.2 | 7.94 ± 0.00 | 1.24 ± 0.00 | 1.92 ± 0.00 |
| | | Dimer | | 8.96 ± 0.04 | 1.40 ± 0.01 | 1.70 ± 0.01 |
| | | Trimer | | 10.9 ± 0.00 | 1.70 ± 0.00 | 1.39 ± 0.00 |
| Isovaleric acid | OV-5 | Monomer | 1108 ± 7 | 9.41 ± 0.04 | 1.47 ± 0.01 | 1.62 ± 0.01 |
| | | Dimer | | 13.2 ± 0.04 | 2.06 ±0 .01 | 1.15 ± 0.00 |
| Methional | OV-5 | Monomer | 207 ± 4 | 7.04 ± 0.04 | 1.09 ± 0.01 | 2.16 ± 0.01 |
| | | Dimer | | 7.90 ± 0.40 | 1.22 ± 0.01 | 1.93 ± 0.01 |
| | | Trimer | | 9.15 ± 0.00 | 1.42 ± 0.00 | 1.66 ± 0.00 |
| 4-Methoxybenzaldehyde | Carbowax 20M | Monomer | 369 ± 3 | 8.28 ± 0.04 | 1.21 ± 0.01 | 1.31 ± 0.01 |
| | | Dimer | | 9.48 ± 0.00 | 1.38 ± 0.00 | 1.14 ± 0.00 |
| | | Trimer | | 11.4 ± 0.00 | 1.67 ± 0.00 | 0.95 ± 0.00 |
| 3-Methylindole | OV-5 | Monomer | 113 ± 2 | 8.17 ± 0.03 | 1.20 ± 0.01 | 1.32 ± 0.01 |
| (E,E)-2,4-Nonadienal | OV-5 | Monomer | 438 ± 24 | 9.29 ± 0.04 | 1.34 ± 0.01 | 1.16 ± 0.01 |
| | | Dimer | | 13.4 ± 0.00 | 1.93 ± 0.00 | 0.81 ± 0.00 |
| 2-Nonanone | OV-5 | Monomer | 136 ± 2 | 9.68 ± 0.00 | 1.40 ± 0.00 | 1.12 ± 0.00 |
| | | Dimer | | 12.9 ± 0.04 | 1.86 ± 0.01 | 0.84 ± 0.00 |
| (E)-2-Nonenal | OV-5 | Monomer | 271 ± 5 | 9.75 ± 0.00 | 1.40 ± 0.00 | 1.11 ± 0.00 |
| | | Dimer | | 10.6 ± 0.04 | 1.53 ± 0.01 | 1.02 ± 0.00 |
| | | Trimer | | 13.6 ± 0.00 | 1.96 ± 0.00 | 0.79 ± 0.00 |
| Octanal | OV-5 | Monomer | 55.5 ± 0.8 | 9.75 ± 0.00 | 1.40 ± 0.00 | 1.11 ± 0.00 |
| | | Dimer | | 10.3 ± 0.00 | 1.48 ± 0.00 | 1.05 ± 0.00 |
| | | Trimer | | 12.6 ± 0.00 | 1.81 ± 0.00 | 0.86 ± 0.00 |
| (E)-2-Octenal | OV-5 | Monomer | 117 ± 3 | 9.20 ± 0.00 | 1.33 ± 0.00 | 1.17 ± 0.00 |
| | | Dimer | | 10.1 ± 0.04 | 1.46 ± 0.01 | 1.07 ± 0.00 |
| | | Trimer | | 12.6 ± 0.10 | 1.82 ± 0.01 | 0.86 ± 0.01 |
| 2-Phenylethanol | Carbowax 20M | Monomer | 238 ± 4 | 8.83 ± 0.04 | 1.30 ± 0.01 | 1.23 ± 0.01 |
| | | Dimer | | 9.41 ± 0.00 | 1.37 ± 0.00 | 1.15 ± 0.00 |
| | | Trimer | | 10.3 ± 0.04 | 1.51 ± 0.01 | 1.05 ± 0.00 |
| Propionic acid | OV-5 | Monomer | 87.0 ± 3.7 | 7.95 ± 0.00 | 1.22 ± 0.00 | 1.92 ± 0.00 |
| | | Dimer | | 10.4 ± 0.00 | 1.60 ± 0.00 | 1.46 ± 0.00 |
| 2-Propanethiol | OV-5 | Monomer | 435 ± 3 | 8.06 ± 0.04 | 1.25 ± 0.01 | 1.89 ± 0.01 |
| | | Dimer | | 9.41 ± 0.04 | 1.46 ± 0.01 | 1.62 ± 0.01 |
| Triethylamine | OV-5 | Monomer | 73.7 ± 4.7 | 7.14 ± 0.04 | 1.01 ± 0.01 | 2.13 ± 0.01 |
| Trimethylamine | OV-5 | Monomer | 18.5 ± 2.2 | 6.12 ± 0.04 | 0.95 ± 0.01 | 2.49 ± 0.02 |
| 2-Undecanone | OV-5 | Monomer | 869 ± 4 | 10.53 ± 0.03 | 1.54 ± 0.01 | 1.03 ± 0.00 |
| | | Dimer | | 11.34 ± 0.03 | 1.66 ± 0.00 | 0.95 ± 0.00 |
| | | Trimer | | 14.32 ± 0.03 | 2.09 ± 0.01 | 0.75 ± 0.00 |
| Valeric acid | OV-5 | Monomer | 1029 ± 11 | 8.98 ± 0.04 | 1.40 ± 0.01 | 1.69 ± 0.01 |
| | | Dimer | | 12.6 ± 0.00 | 1.97 ± 0.00 | 1.21 ± 0.00 |

RIP ($Ko_{(RIP)}$) in the nitrogen buffer gas system was experimentally determined to be $2.36 \pm 0.04\ cm^2\ V^{-1}\ s^{-1}$ ($n = 30$)).

### 3.3. Volatile Compound Analysis

The identification of VCs was performed using standards diluted with water, for each compound the identification was repeated three times. The results for drift time, retention time, relative drift time and reduced ion mobility are presented in Table 2. In most cases, the product ions are formed through ionisation processes that have lower reduced ion mobility values (i.e. higher drift time and relative retention times) than the RIP (i.e. $Ko_{(RIP)} = 2.36 \pm 0.04\ cm^2\ V^{-1}\ s^{-1}$), except in the causes of ammonia, trimethyl amine and dimethyl sulphide. Compounds, which have relative drift times <1, form a gaseous analyte molecule have to be smaller than the water containing positive reactant ion $H_3O^+(H_2O)_{m-2}$.

As IMS distinguishes ions on the basis of differences in mass, charge and collision cross-sectional area, it is possible to separate and identify isomeric compounds with good resolution [1]. In this work, two sets of isomeric organic acids (butyric acid: isobutyric acid and valeric acid: isovaleric acid) have been successfully separated by IMS (see Table 2). In addition, the reduced ion mobility of sulphides decreases as the number of sulphur atoms increases, that is, dimethyl sulphide $2.47\ cm^2\ V^{-1}\ s^{-1}$; dimethyl disulphide $2.05\ cm^2\ V^{-1}\ s^{-1}$ and dimethyl trisulphide $1.77\ cm^2\ V^{-1}\ s^{-1}$. This gradual decrease in ion mobility indicates a higher ionic mass of product ions formed for these sulphides. Similarly, the same effect can be seen for the *n*-alkyl organic acids in which the reduced ion mobility decreases as the number of carbon atoms increases, that is, propionic acid ($1.92\ cm^2\ V^{-1}\ s^{-1}$ for the monomer), butyric acid ($1.87\ cm^2\ V^{-1}\ s^{-1}$ for the monomer) and hexanoic acid ($1.64\ cm^2\ V^{-1}\ s^{-1}$ for the monomer; Table 2). In addition, many VCs indicate the formation of different product ions with the highest reduced ion mobility for the monomer and the lowest for the trimer, whereas small tertiary amines, that is, trimethylamine and triethylamine, provide well-defined separation which consists of two single product ion peaks (Fig. 4); unfortunately the small nitrogen compounds tend to form resultant tailing peaks.

Calibration graphs were established for all VCs under the operating conditions shown in Supplementary Information. In generic terms, the sum of the blank corrected peak intensity was plotted for the monomer and any subsequent dimer and trimer against the mass of VC (see Fig. 5). A range of linear and non-linear relationships were obtained for the calibration plots (see Supplementary Information). For quantitative analysis, only the linear portion of the calibration plot was used and these are reported in Table 3. In addition, the LOD, based on three times the standard deviation of the background, and limit of quantification, based on 10 times the standard deviation of the background, are reported (Table 3). Generally, the detection limits ranged from 0.1 ng (bis(methylthio)methane, ethylbutanoate and (E)-2-nonenal) to 472 ng (isovaleric acid). The highest detection limits were achieved for the acid compounds, that is, butyric acid (9.0 ng), hexanoic acid (60 ng), isobutyric acid (67 ng), isovaleric acid (472 ng), propionic acid (203 ng) and valeric acid (65 ng). In addition, the linear dynamic range and its associated regression coefficient ($R^2$) for each VC are reported, except triethylamine and trimethylamine for which no acceptable data were obtained (Table 3). Correlation coefficient ($R^2$) data ranged from to 0.9793 (for the dimer of octanal) through to 0.9990 (for isobutyric acid).

### 3.4. Sample Analysis

Socks were chosen as the sample matrix from which to investigate the occurrence of malodour and the key VCs associated with it. Initial studies sought to investigate the potential matrix effects that different, but generically available, socks might make on the recoveries of VCs. To facilitate this eight VCs were selected to investigate, namely butyric acid, dimethyl disulphide, dimethyl trisulphide, ethanethiol, hexanoic acid, isobutyric acid, 2-propanethol and valeric acid; standard solutions of the VCs were prepared, within their own pre-determined linear dynamic range (based on data reported in Table 3), and then spiked onto an inert matrix, that is, filter paper, and two different sock types. In each case, an approximate 0.5 g sample mass was maintained for the sock samples; all experimental determinations were done in triplicate. The percentage recoveries for each VC are shown in Table 4. Acceptable recoveries (in the range 72–132%) was obtained from the inert filter paper matrix with an average recovery of $101 \pm 18\%$ ($n = 8$). However, in general terms, lower recoveries were obtained from the sock analyses. The average recovery from sock type 1 (i.e. 74% cotton, 19% polyester, 5% nylon and 2% lycra) was $54 \pm 30\%$ ($n = 8$) while from sock type 2 (i.e. 74% cotton, 25% polyester and 1% elastane) it was $78 \pm 24\%$ ($n = 6$). As a result, any subsequent analysis will only at best provide a precise estimate of the mass of VC present.

A human volunteer study was then done in which 11 participants (seven male and four female) were invited to wear new socks for a minimum of 10 h per day in their chosen footwear. This was repeated three times over a 3-week period. Upon collection of the socks, they were olfactory graded for malodour against a fixed scale (0–10) prior to SHS-MCC-GC-IMS analysis. No discernible malodour grading difference, per individual, was noted between the left and right socks; therefore, the average malodour grade was reported alongside the outer footwear type (Table 5). It was noted from the analysis of unworn (blank) sock samples that a number of background compounds were present; as a result all samples analysed were subjected to background subtraction. In addition, an impurity peak was identified at the retention time of 1107 s ($Ko_{(VC)} = 1.62\ cm^2\ V^{-1}\ s^{-1}$) which interfered with the identification, and hence any confirmation, of isovaleric acid (monomer).

By comparison with the SHS-MCC-GC-IMS database library (Table 2 and Fig. 4), it was possible to identify four VCs in the soiled sock sample odour profiles. The most abundant VCs in the odour profiles, irrespective of gender, were ammonia and dimethyl disulphide with minor components of dimethyl trisulphide and butyric acid identifiable. Ammonia was detected in all samples at high concentration (beyond the extended calibration range) at a drift time of 5.72 ms and a $Ko_{(VC)}$ of $2.66\ cm^2\ V^{-1}\ s^{-1}$. In addition, a range of other VCs were present in the sample chromatograms which could not be assigned to a specific VC based on the current database. However, compilation of the co-ordinates for the unknown VCs would allow confirmation in future as the database is expanded. A summary of the quantification data for dimethyl disulphide, dimethyl trisulphide and butyric acid from the sock analyses is shown in Table 5.

In addition to the presence of high ammonia concentrations, dimethyl disulphide was also determined at high concentration coincident with a high malodour grading, that is, $\geq 6$ with a mean value of $7.16\ \mu g\ g^{-1}$, $6.97\ \mu g\ g^{-1}$, $8.80\ \mu g\ g^{-1}$, $5.64\ \mu g\ g^{-1}$ in volunteer samples A (week 2), E (week 3), H (week 3) and J (week 2), respectively. In contrast, dimethyl disulphide was not detected (on the basis of LOQ data) for volunteer D (week 1), I (week 1), J (week 1) and K (week 1) which all had corresponding olfactory grading for malodour of 2. No similar link was identified between the olfactory grading malodour profile and the determination of either dimethyl trisulphide or butyric acid.

Statistical analysis was also done to investigate whether there was any statistical difference between the occurrence of dimethyl disulphide and the gender. Statistical evaluation was done using a two-tailed *t* test, with a *p* value of 0.05 for the 95% confidence level.

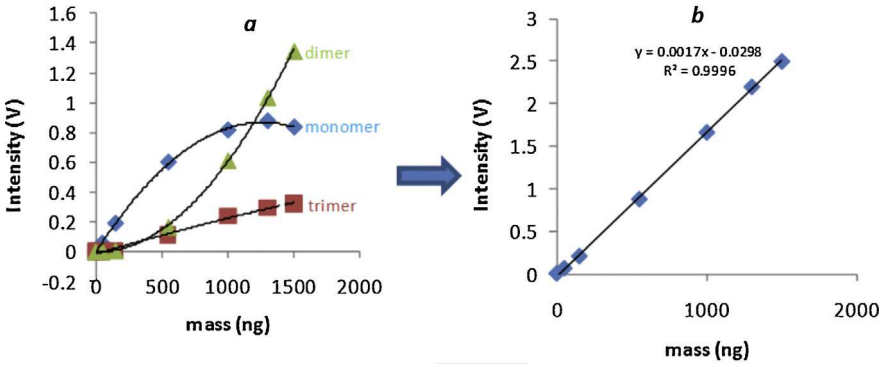


**Fig. 5.** (A) Individual calibration curves of monomer, dimer and trimer and (B) sum of intensities of monomer, dimer and trimer for 2-phenylethanol.

**Table 3**
Calibration data for all compounds by SHS-MCC-GC-IMS.

| Compound | Column type | Compound cluster | Effective linear range (ng) | Equation for the effective linear range | $R^2$ | LOD (ng) | LOQ (ng) |
|---|---|---|---|---|---|---|---|
| Ammonia | Carbowax 20M | Monomer | 0–1000 | $y = 0.0032x - 0.0124$ | 0.9986 | 8.0 | 26 |
| Bis(methylthio)methane | OV-5 | Monomer + dimer | 0–10 | $y = 0.1634x + 0.1141$ | 0.9841 | 0.1 | 0.4 |
| 1-Butanethiol | OV-5 | Monomer + dimer | 0–100 | $y = 0.0112x + 0.0225$ | 0.9952 | 0.9 | 2.9 |
| Butyric acid | OV-5 | Monomer + dimer + trimer | 0–2000 | $y = 0.0003x + 0.0098$ | 0.9947 | 9.0 | 30 |
| (E,E)-2,4-Decadienal | OV-5 | Monomer + dimer | 0–100 | $y = 0.0141x - 0.0113$ | 0.9902 | 3.1 | 10 |
| 1-Decanol | Carbowax 20M | Monomer + dimer | 0–200 | $y = 0.0035x + 0.0242$ | 0.9902 | 8.5 | 28 |
| Dimethyl disulphide | OV-5 | Monomer | 0–6000 | $y = 0.0006x - 0.1293$ | 0.9900 | 74 | 248 |
| Dimethyl sulphide | OV-5 | Monomer | 0–900 | $y = 0.0021x + 0.1039$ | 0.9858 | 60 | 199 |
| Dimethyl trisulphide | OV-5 | Monomer | 0–100 | $y = 0.0065x - 0.0283$ | 0.9812 | 3.0 | 9.0 |
| 1-Dodecanol | Carbowax 20M | Monomer + dimer | 0–300 | $y = 0.0018x - 0.0072$ | 0.9989 | 16 | 53 |
| Ethanethiol | OV-5 | Monomer + dimer | 0–300 | $y = 0.0057x + 0.01$ | 0.9977 | 6.3 | 21 |
| Ethylbutanoate | OV-5 | Monomer + dimer + trimer | 0–5 | $y = 0.5272x + 0.0516$ | 0.9926 | 0.1 | 0.4 |
| 4-Fluoroacetophenone | OV-5 | Monomer + dimer + trimer | 0–200 | $y = 0.0089x - 0.0315$ | 0.9906 | 8.3 | 14 |
| Guaiacol | Carbowax 20M | Monomer + dimer + trimer | 0–200 | $y = 0.0114x - 0.0063$ | 0.9900 | 1.5 | 5.0 |
| Hexanoic acid | OV-5 | Monomer + dimer | 0–2000 | $y = 0.0002x + 0.0148$ | 0.9906 | 60 | 201 |
| Isobutyric acid | OV-5 | Monomer + dimer + trimer | 0–2000 | $y = 0.0004x + 0.0118$ | 0.9990 | 67 | 223 |
| Isovaleric acid | OV-5 | Monomer + dimer | 0–1000 | $y = 8e^{-5}x + 0.0107$ | 0.9933 | 472 | 1573 |
| Methional | OV-5 | Monomer + dimer + trimer | 0–350 | $y = 0.0067x - 0.0366$ | 0.9831 | 5.0 | 17 |
| 4-Methoxybenzaldehyde | Carbowax 20M | Monomer + dimer + trimer | 0–350 | $y = 0.004x - 0.0453$ | 0.9945 | 3.8 | 13 |
| 3-Methylindole | OV-5 | Monomer | 0–150 | $y = 0.0056x + 0.0038$ | 0.9835 | 13 | 42 |
| (E,E)-2,4-Nonadienal | OV-5 | Monomer + dimer | 0–20 | $y = 0.0086x + 0.0802$ | 0.9961 | 0.6 | 2.1 |
| 2-Nonanone | OV-5 | Dimer[a] | 0–50 | $y = 0.0335x + 0.0867$ | 0.9803 | 0.3 | 1.0 |
| (E)-2-Nonenal | OV-5 | Monomer + dimer + trimer | 0–30 | $y = 0.0288x + 0.0085$ | 0.9961 | 0.1 | 0.4 |
| Octanal | OV-5 | Dimer[a] | 0–100 | $y = 0.0066x + 0.0306$ | 0.9793 | 0.7 | 9.4 |
| (E)-2-Octenal | OV-5 | Monomer + dimer + trimer | 0–100 | $y = 0.0048x + 0.1915$ | 0.9904 | 0.6 | 1.9 |
| 2-Phenylethanol | Carbowax 20M | Monomer + dimer + trimer | 0–1500 | $y = 0.0017x - 0.0298$ | 0.9996 | 6.4 | 21 |
| Propionic acid | OV-5 | Monomer + dimer | 0–5000 | $y = 0.0002x + 0.0119$ | 0.9951 | 203 | 678 |
| 2 Propanethiol | OV-5 | Monomer + dimer | 0–100 | $y = 0.0299x + 0.199$ | 0.9847 | 1.0 | 3.0 |
| Triethylamine | OV-5 | Monomer | ND | | | | |
| Trimethylamine | OV-5 | Monomer | ND | | | | |
| 2-Undecanone | OV-5 | Monomer + dimer + trimer | 0–650 | $y = 0.0013x + 0.0334$ | 0.9802 | 23 | 7.6 |
| Valeric acid | OV-5 | Monomer + dimer | 0–8000 | $y = 9e^{-5}x + 0.0205$ | 0.9955 | 65 | 215 |

[a] For these compounds, due to the poor linearity of the monomer and subsequent sum of the intensities only the dimer has been considered and used for the quantification.

**Table 4**
Percentage recoveries[a] for eight compounds using SHS-MCC-GC-IMS[b].

| Compound | Spiked concentration (ng) | Percentage recoveries ($n = 3$) | | |
|---|---|---|---|---|
| | | Filter paper[c] | Sock type 1[d] | Sock type 2[e] |
| Butyric acid | 1500 | 103 ± 3 | 59 ± 7 | 101 ± 26 |
| Dimethyl disulphide | 3000 | 72 ± 28 | 58 ± 16 | ND |
| Dimethyl trisulphide | 100 | 91 ± 4 | 64 ± 11 | 85 ± 7 |
| Ethanethiol | 300 | 132 ± 11 | 74 ± 9 | 72 ± 3 |
| Hexanoic acid | 8000 | 117 ± 2 | 34 ± 4 | 58 ± 9 |
| Isobutyric acid | 3000 | 108 ± 14 | 32 ± 5 | ND |
| 2-Propanethiol | 80 | 94 ± 3 | 39 ± 5 | 57 ± 8 |
| Valeric acid | 8000 | 94 ± 5 | 68 ± 12 | 96 ± 2 |

[a] 100 μL of a multicompound mixture was used for calibration; filter paper or sock sample was placed in the 20 mL vial for sampling.
[b] MCC-IMS conditions: sample incubation time, 5 min; sample incubation temperature, 95 °C; syringe temperature, 85 °C; injection volume, 1.5 mL; column, OV-5; column temperature, 35 °C; carrier gas flow rate, 10 mL min$^{-1}$; drift gas flow rate 500 mL min$^{-1}$; IMS temperature, 60 °C; and, RIP voltage, positive mode.
[c] 0.015 g.
[d] 0.50 g sock type 1.
[e] 0.50 g sock type 2.
ND = VCs not determined due to background interference.

**Table 5**
Sock analysis using olfactory grading[a] and SHS-MCC-GC-IMS[b] (ng/g).

| Code A Male | | | Code B Female | | | Code C Male | | |
|---|---|---|---|---|---|---|---|---|
| *Week 1* | *Week 2* | *Week3* | *Week 1* | *Week2* | *Week 3* | *Week 1* | *Week 2* | *Week 3* |
| FWT: shoe | FWT: shoe | FWT: shoe | FWT: shoe | FWT: shoe | FWT: shoe | FWT: shoe | FWT: shoe | FWT: shoe |
| OG: 4 | OG: 7 | OG: 5 | OG: 5 | OG: 5 | OG: 3 | OG: 4 | OG: 4 | OG: 5 |
| DMDS = 4876 ± 1272 | DMDS = 7160 ± 344 | DMDS = 7726 ± 1673 | DMDS = 5070 ± 2039 | DMDS = 935 ± 489 | DMDS = 991 ± 325 | DMDS = 1049 ± 431 | DMDS = 1633 ± 628 | DMDS = 2324 ± 716 |
| DMTS = 100 ± 6 | DMTS = 40 ± 5 | DMTS = 82 ± 16 | DMTS = 99 ± 4 | DMTS = 76 ± 10 | DMTS = 120 ± 22 | DMTS = 101 ± 1.3 | DMTS = 71 ± 10.1 | DMTS = 58 ± 8 |
| BA = ND | BA = ND | BA = ND | BA = ND | BA = 911 ± 855 | BA = 236 ± 130 | BA = 927 ± 268 | BA = ND | BA = 1272 ± 271 |
| Code D Female | | | Code E Male | | | Code F Male | | |
| *Week 1* | *Week 2* | *Week 3* | *Week 1* | *Week 2* | *Week 3* | *Week 1* | *Week 2* | *Week 3* |
| FWT: slipper | FWT: shoe | FWT: shoe | FWT: shoe | FWT: shoe | FWT: shoe | FWT: shoe | FWT: shoe | FWT: shoe |
| OG: 2 | OG: 3 | OG: 3 | OG: 5 | OG: 5 | OG: 7 | OG: 3 | OG: 4 | OG: 4 |
| DMDS = ND | DMDS = 456 ± 202 | DMDS = 693 ± 457 | DMDS = 1432 ± 307 | DMDS = 2232 ± 946 | DMDS = 6972 ± 510 | DMDS = 530 ± 507 | DMDS = 2010 ± 1125 | DMDS = 2714 ± 1620 |
| DMTS = 108 ± 5 | DMTS = 70 ± 18 | DMTS = 67 ± 8 | DMTS = 97 ± 0.5 | DMTS = 68 ± 2 | DMTS = 62 ± 31 | DMTS = 107 ± 6 | DMTS = 123 ± 42 | DMTS =130 ± 51 |
| BA = 232 ± 137 | BA = ND | BA = 1090 ± 525 | BA = 406 ± 130 | BA = ND | BA = 1186 ± 141 | BA = 284 ± 233 | BA = 1080 ± 520 | BA = 335 ± 279 |
| Code G Male | | | Code H Female | | | Code I Female | | |
| *Week 1* | *Week 2* | *Week 3* | *Week 1* | *Week 2* | *Week 3* | *Week 1* | *Week 2* | *Week 3* |
| FWT: shoe | FWT: shoe | FWT: shoe | FWT: shoe | FWT: shoe | FWT: shoe | FWT: slipper | FWT: shoe | FWT: shoe |
| OG: 3 | OG: 4 | OG: 5 | OG: 4 | OG: 5 | OG: 6 | OG: 2 | OG: 3 | OG: 3 |
| DMDS = 2071 ± 597 | DMDS = 2067 ± 704 | DMDS= 1532 ± 461 | DMDS = 4133 ± 2043 | DMDS = 5842 ± 799 | DMDS = 8801 ± 517 | DMDS = ND | DMDS = 522 ± 213 | DMDS = 1168 ± 329 |
| DMTS = 106 ± 4 | DMTS = 94 ± 9 | DMTS = 94 ± 13 | DMTS = 109 ± 3 | DMTS = 82 ± 14 | DMTS = 107 ± 22 | DMTS = 100 ± 2 | DMTS = 69 ± 1.2 | DMTS =78 ± 15 |
| BA =596 ± 160 | BA = ND | BA = 236 ± 207 | BA = 145 ± 133 | BA = 958 ± 674 | BA = 441 ± 170 | BA = 280 ± 198 | BA= ND | BA = 580 ± 288 |
| Code J Male | | | Code K Female | | | | | |
| *Week 1* | *Week 2* | *Week 3* | *Week 1* | *Week 2* | *Week 3* | | | |
| FWT: slipper | FWT: shoe | FWT: shoe | FWT: slipper | FWT: slipper, shoe | FWT: shoe | | | |
| OG: 2 | OG: 6 | OG: 5 | OG: 2 | OG: 3 | OG: 4 | | | |
| DMDS = ND | DMDS = 5636 ± 2402 | DMDS = 6999 ± 898 | DMDS = ND | DMDS = 590 ± 82 | DMDS = 491 ± 145 | | | |
| DMTS = 113 ± 4 | DMTS = 242 ± 37 | DMTS = 238 ± 26 | DMTS = 104 ± 1 | DMTS = 56 ± 11 | DMTS = 170 ± 28 | | | |
| BA = ND | BA = ND | BA = ND | BA = 606 ± 172 | BA = ND | BA = 812 ± 315 | | | |

[a] OG malodour grading scale: 0, no malodour; 2–3, believe there is malodour; 4–5, there is malodour; 6–7, malodour is strong; 8–9, malodour is very strong; 10, malodour is extreme.

[b] SHS-MCC-GC-IMS values reported in ng/g. Ammonia was determined in all sock samples irrespective of gender or duration; however, it was not possible to quantify due to its excessive concentration. DMDS, dimethyl disulphide; DMTS, dimethyl trisulphide; BA, butyric acid.

It was found that there was no statistical significant difference in the malodour in the socks of male and female participants.

## 4. Conclusions

SHS-MCC-GC-IMS has been fully evaluated for the identification of volatile compounds and specifically ammonia- and sulphur-related compounds. Based on the optimisation of the key operating parameters, a database was developed that subsequently allowed the identification of four volatile compounds in soiled sock samples. Further work is required to extend the current database and apply the approach to other sample types and matrices.

## Acknowledgement

The authors are grateful for funding for the project from Procter and Gamble, Newcastle Innovation Centre, Newcastle upon Tyne and Northumbria University (Research Development Fund).

## Appendix A. Supplementary data

Supplementary data associated with this article can be found, in the online version, at http://dx.doi.org/10.1016/j.chroma.2014.02.047.

## References

[1] R.M. O'Donnell, X. Sun, P.D.B. Harrington, Trends Anal. Chem. 27 (2008) 44.
[2] J.S. Babis, R.P. Sperline, A.K. Knight, D.A. Jones, C.A. Gresham, M.B. Denton, Anal. Bioanal. Chem. 395 (2009) 411.
[3] M.A. Mäkinen, O.A. Anttalainen, M.E.T. Sillanpää, Anal. Chem. 82 (2010) 9594.
[4] S. Zimmermann, S. Barth, W.K.M. Baether, J. Ringer, Anal. Chem. 80 (2008) 6671.
[5] R.G. Ewing, D.A. Atkinson, G.A. Eiceman, E.J. Ewing, Talanta 54 (2001) 515.
[6] R. Garrido-Delgado, L. Arce, M. Valcárcel, Anal. Bioanal. Chem. 402 (2012) 489.
[7] T. Perl, B. Bödeker, M. Jünger, J. Nolte, W. Vautz, Anal. Bioanal. Chem. 397 (2010) 2385.
[8] E.S. Baker, A.A. Schepmoes, D.F. Hopkins, K. Tang, R.D. Smith, M.E. Belov, E.A. Livesay, D.J. Orton, R.J. Moore, r.W.F. Danielson, D.C. Prior, Y.M. Ibrahim, B.L. LaMarche, A.M. Mayampurath, J. Proteome Res. 9 (2010) 997.
[9] S.J. Valentine, X. Liu, M.D. Plasencia, A.E. Hilderbrand, R.T. Kurulugama, S.L. Koeniger, D.E. Clemmer, Exp. Rev. Proteomics 2 (2005) 553.
[10] W.E. Steiner, W.A. English, J.H.H. Hill, J. Phys. Chem. A 110 (2006) 1836.
[11] W.E. Steiner, C.S. Harden, F. Hong, S.J. Klopsch, J.H.H. Hill, V.M. McHugh, J. Am. Soc. Mass Spectrom. 17 (2006) 241.
[12] W. Vautz, B. Bödeker, J.I. Baumbach, S. Bader, M. Westhoff, T. Perl, Int. J. Ion Mob. Spectrom. 12 (2009) 47.
[13] V. Ruzsanyi, J.I. Baumbach, S. Sielemann, P. Litterst, M. Westhoff, L. Freitag, J. Chromatogr. A 1084 (2005) 145.
[14] A.B. Kanu, J.H.H. Hill, J. Chromatogr. A 1177 (2008) 12.
[15] H. Borsdorf, K. Neitsch, Int. J. Ion Mob. Spectrom. 12 (2009) 39.
[16] M. Tabrizchi, E. Khezri, Int. J. Ion Mob. Spectrom. 11 (2008) 19.
[17] V. Ruzsanyi, P. Mochalski, A. Schmid, H. Wiesenhofer, M. Klieber, H. Hinterhuber, A. Amann, J. Chromatogr. B 911 (2012) 84.
[18] M. Jünger, W. Vautz, M. Kuhns, L. Hofmann, S. Ulbricht, J.I. Baumbach, M. Quintel, T. Perl, Appl. Microbiol. Biotechn. 93 (2012) 2603.
[19] Z. Karpas, O. Litvin, G. Cohen, J. Mishin, E. Atweh, A. Burlakov, Int. J. Ion Mob. Spectrom. 14 (2011) 3.
[20] M. Westhoff, P. Litterst, L. Freitag, W. Urfer, S. Bader, J.I. Baumbach, Thorax 64 (2009) 744.
[21] R. Garrido-Delgado, L. Arce, A.V. Guamán, A. Pardo, S. Marco, M. Valcárcel, Talanta 84 (2011) 471.
[22] D. Zamora, M. Alcalà, M. Blanco, Anal. Chim. Acta 708 (2011) 69.
[23] H. Tong, N. Sze, B. Thomson, S. Nacson, J. Pawliszyn, Analyst 127 (2002) 1207.
[24] T. Kotiaho, F.R. Lauritsen, H. Degn, H. Paakkanen, Anal. Chim. Acta 309 (1995) 317.
[25] T. Perl, M. Jünger, W. Vautz, J. Nolte, M. Kuhns, M. Borg-von Zepelin, M. Quintel, Mycoses 54 (2011) e828.
[26] H. Kubota, A. Mitani, Y. Niwano, K. Takeuchi, A. Tanaka, N. Yamaguchi, Y. Kawamura, J. Hitomi, App. Environ. Microbiol. 78 (2012) 3317.
[27] S. Munk, C. Johansen, L.H. Stahnke, J. Adler-Nissen, J. Surfactants Deterg. 4 (2001) 385.
[28] Y. Nagoh, S. Tobe, T. Watanabe, T. Mukaiyama, Tenside Surfactants Deterg. 42 (2005) 7.
[29] K. Takeuchi, Y. Hasegawa, H. Ishida, M. Kashiwagi, Flav. Fragr. J. 27 (2012) 89.
[30] T. Akutsu, K. Sekiguchi, T. Ohmori, K. Sakurada, Chem. Senses 31 (2006) 557.
[31] Y. Hasegawa, M. Yabuki, M. Matsukane, Chem. Biodiv. 1 (2004) 2042.
[32] S. Munk, P. Münch, L. Stahnke, J. Adler-Nissen, P. Schieberle, J. Surfactants Deterg. 3 (2000) 505.
[33] K. Stapleton, K. Hill, K. Day, J.D. Perry, J.R. Dean, Lett. Appl. Microbiol. 56 (2013) 299.
[34] G. Eiceman, Z. Karpas, Ion Mobility Spectrometry, CRC Press, 2005 (ISBN 0-8493-2247-2).
[35] S. Konig, H.M. Fales, Am. Soc. Mass Spectrom. 9 (1998) 814.
[36] G. Hulthe, G. Stenhagen, O. Wennerstrom, C.-H. Ottosson, J. Chromatogr. A 777 (1997) 155.
[37] C. Tiebe, T. Hübert, B. Koch, U. Ritter, I. Stephan, Int. J. Ion Mob. Spectrom. 13 (2010) 17.
[38] C. Tiebe, H. Miessner, B. Koch, T. Hübert, Anal. Bioanal. Chem. 395 (2009) 2313.